Crucial Structural Factors and Mode of Action of Polyene Amides as Inhibitors for Mitochondrial NADH−Ubiquinone Oxidoreductase (Complex I)†

Takehiko Yoshida, Masatoshi Murai, Masato Abe, Naoya Ichimaru, Toshiyuki Harada, Takaaki Nishioka, and Hideto Miyoshi*

Division of Applied Life Sciences, Graduate School of Agriculture, Kyoto University, Sakyo-ku, Kyoto 606-8502, Japan

Received May 26, 2007; Revised Manuscript Received July 1, 2007

ABSTRACT: Natural antibiotic polyene amides such as myxalamides are potent inhibitors of mitochondrial complex I. Because of the significant instability of this series of compounds due to an extended π-conjugation skeleton, a detailed characterization of their inhibitory action has not been performed. To elucidate the action mechanism as well as binding manner of polyene amides with complex I, identification of the roles of each functional group in the inhibitory action is needed. We here synthesized a series of amide analogues and carried out structure−activity studies with bovine heart mitochondrial complex I. With respect to the left-hand portion, the natural π-conjugation skeleton common to many natural products is not required for the inhibition and can be substituted with a simpler substructure such as a conjugated diene. The geometry and shape of the left-hand portion were shown to be important for the inhibition, suggesting that this portion may bind to a narrow hydrophobic pocket in the enzyme rather than merely partitioning into the lipid membrane phase. Concerning the right-hand portion of the inhibitor, the presence of the 2-methyl, amide NH, and (*S*)-1′-methyl groups was crucial for the activity, suggesting that both methyl groups neighboring the amide group finely adjust the hydrogen-bonding ability of the amide group. In contrast, modifications of the 2′-OH group did not significantly influence the activity, suggesting that the role of this functional group is not to serve as a hydrogen bond donor to the enzyme but to act as a hydrophilic anchor directing the right-hand portion at or near the membrane surface. Detailed characterization of the action mechanism indicated that the polyene amides share a common binding domain with other complex I inhibitors, though their binding position (or manner) within the domain may differ considerably from that of other inhibitors.

Natural antibiotic polyene amides, such as myxalamides A−D and stipiamide (Figure 1), are a group of metabolites produced by myxobacteria and exhibit potent insecticidal and antifungal activities (*1*−*3*). These biological activities are thought to be attributable to the inhibition of mitochondrial NADH−ubiquinone oxidoreductase (complex I)[1] (*1*−*3*), which catalyzed the oxidation of NADH by ubiquinone, coupled to the generation of an electrochemical proton gradient across the inner mitochondrial membrane (*4*). Polyene amides were first shown to be inhibitors of mitochondrial complex I in 1983 by Reichenbach's group (*1*), but a detailed characterization of the action mechanism of this series of inhibitors has yet to be performed since the amides are very unstable during isolation or preparation conditions due to a largely extended π-conjugation system, and hence long-term storage under air leads to substantial loss of material (*2*, *5*−*7*). In particular, a C6/C7 *Z* double bond, which is a structural feature common to natural polyene amides, isomerizes readily to a more stable *E* double bond (*5*−*8*). Taking into consideration this characteristic, the question of whether past studies (*1*, *9*) on the inhibition of complex I using natural polyene amides really evaluated the activity of pure individual samples would be posed.

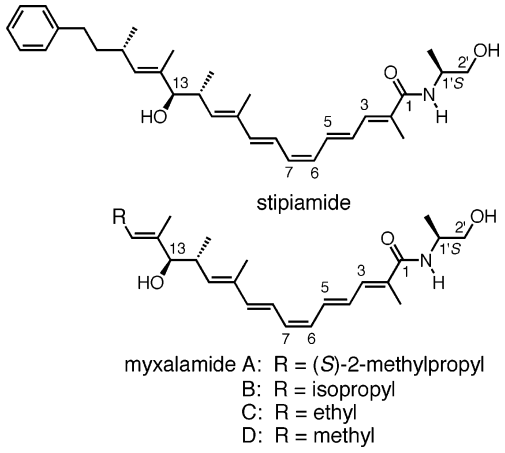

FIGURE 1: Structures of natural polyene amides (stipiamide and four myxalamide derivatives).

† This work was supported in part by a Grant-in-aid for Scientific Research from the Japan Society for the Promotion of Science (Grant 17380073 to H.M.).

* To whom correspondence should be addressed: e-mail, miyoshi@kais.kyoto-u.ac.jp; tel, +81-75-753-6119; fax, +81-75-753-6408.

[1] Abbreviations: complex I, mitochondrial proton-pumping NADH−ubiquinone oxidoreductase; complex III, cytochrome bc_1 complex; MDR, multidrug resistance; NOE, nuclear Overhauser effect; Q_o site, ubiquinol oxidation site in the cytochrome bc_1 complex; SAR, structure−activity relationship; SDS−PAGE, sodium dodecyl sulfate−polyacrylamide gel electrophoresis; SMP, submitochondrial particles; [^{125}I]TDA, [^{125}I](trifluoromethyl)phenyl*di*azirinyl*ac*etogenin.

10.1021/bi7010306 CCC: $37.00
Published on Web 08/09/2007

The long conjugated polyene skeleton of the amides is very unique among complex I inhibitors. Accordingly, a detailed analysis of their action mechanism may provide useful insight into the inhibitor-binding site(s) in complex I, which is believed to be closely associated with the functionality of the membrane segment such as ubiquinone reduction and proton pumping (*10*−*12*). To elucidate the action mechanism as well as binding manner of the polyene amides with mitochondrial complex I, identification of structural factors crucial to the inhibition is needed, as we have reported for other complex I inhibitors such as capsaicins (*13*, *14*), rotenoids (*15*, *16*), and acetogenins (*17*−*19*). Moreover, it is noteworthy that some synthetic polyene amide derivatives reverse P-glycoprotein-mediated multidrug resistance (MDR) with MCF-7adrR breast cancer cells by directly binding to P-glycoprotein (*20*−*22*). When the therapeutic use of the amide derivatives as MDR reversing agents or P-glycoprotein modulators is considered (*21*−*23*), identification of the crucial structural factors is also valuable to rationally reduce their inherent cytotoxicity due to the inhibition of complex I. Therefore, we synthesized a series of polyene amides and carried out a structure−activity relationship (SAR) study for the inhibition of bovine heart mitochondrial complex I. This study provides the first detailed characterization of polyene amides as complex I inhibitors.

EXPERIMENTAL PROCEDURES

Synthesis of Test Compounds. A series of polyene amide inhibitors synthesized in this study are shown in Figure 2. The synthetic procedures are described in the Supporting Information. The geometry of the disubstituted olefins was determined from the coupling constants of the olefin protons in the ^{1}H NMR spectra (*3*). The *E* geometry of the trisubstituted olefin at C2 was determined from the nuclear Overhauser effect (NOE) of H4/2-Me protons (*3*). The photoreactive acetogenin derivative [^{125}I](*t*rifluoromethyl)-phenyl*d*iazirinyl*a*cetogenin ([^{125}I]TDA), used for photoaffinity labeling of the ND1 subunit, is the same sample as used previously (*24*).

Measurement of Complex I Activity. Bovine heart submitochondrial particles (SMP) were prepared by the method of Matsuno-Yagi and Hatefi (*25*) using a sonication medium containing 0.25 M sucrose, 1 mM succinate, 1.5 mM ATP, 10 mM $MgCl_2$, 10 mM $MnCl_2$, and 10 mM Tris-HCl (pH 7.4) and stored in a buffer containing 0.25 M sucrose and 10 mM Tris-HCl (pH 7.4) at −84 °C. The NADH oxidase activity in SMP was followed spectrometrically with a Shimadzu UV-3000 (340 nm, $\epsilon = 6.2$ mM^{-1} cm^{-1}) at 25 °C. The reaction medium (2.5 mL) contained 0.25 M sucrose, 1 mM $MgCl_2$, and 50 mM phosphate buffer (pH 7.5). The final mitochondrial protein concentration was 30 μg of protein/mL. The reaction was started by adding 50 μM NADH after the equilibration of SMP with an inhibitor for 4 min.

Measurement of Superoxide Production. Superoxide production was determined at 25 °C by monitoring the superoxide-dependent oxidation of epinephrine to adrenochrome (*26*) with a Shimadzu UV-3000 spectrophotometer (485−575 nm, $\epsilon = 3.0$ mM^{-1} cm^{-1}) in a dual wavelength mode. The reaction medium (2.5 mL) contained 0.25 M sucrose, 1 mM epinephrine, 1 mM EDTA, 1 μM catalase, and 10 mM Tris-HCl buffer (pH 7.5). The reaction was started by adding 100 μM NADH after the equilibration of SMP with the test inhibitor for 4 min. The final protein concentration of SMP was 0.25 mg/mL. Superoxide dismutase (bovine liver) was used at a final concentration of 60 units/mL to give the assay specificity.

Measurement of Reverse Electron Transfer. Reverse electron transfer (ubiquinol−NAD^+ oxidoreductase activity) was generated by the oxidation of succinate and the hydrolysis of ATP (*27*). The reaction was measured spectrometrically by following the reduction of NAD^+ with a Shimadzu UV-3000 (340 nm, $\epsilon = 6.2$ mM^{-1} cm^{-1}) at 25 °C. The reaction medium (2.5 mL) contained 0.25 M sucrose, 7 mM sodium succinate, 6 mM $MgCl_2$, 1 mM KCN, 1 mM NAD^+, and 50 mM Tris-HCl (pH 7.5), and the final protein concentration of SMP was 0.1 mg of protein/mL. The reaction was started by the addition of 2 mM ATP after the equilibration of SMP with an inhibitor for 4 min. The activity was fully sensitive to SF6847 (protonophoric uncoupler) or oligomycin (ATP synthase inhibitor) (*27*).

Photoaffinity Labeling of the ND1 Subunit by [^{125}I]TDA. Photoaffinity labeling of the ND1 subunit by an acetogenin derivative [^{125}I]TDA was carried out as described previously (*24*). In brief, SMP (0.3 mg of protein/mL) in 100 μL of buffer containing 250 mM sucrose, 1 mM $MgCl_2$, and 50 mM phosphate (pH 7.4) were treated with [^{125}I]TDA (3 nM) in 1.5 mL Eppendorf tubes and incubated for 10 min at room temperature. The samples were then irradiated with a long-wavelength UV lamp (Black-Ray model B-100A, UVP) for 10 min on ice at a distance of 10 cm from the light source. When a replacement test was carried out, a competitor (i.e., other inhibitors) was added and incubated for 10 min at room temperature prior to the treatment with [^{125}I]TDA.

SDS−PAGE was performed according to Laemmli (*28*). Briefly, [^{125}I]TDA-labeled SMP samples were added to 4× sample buffer and incubated at 35 °C for 1 h to prevent protein aggregation. These denatured samples were separated on 10−20% gradient gels (90 × 83 × 1 mm). About 4−6 μg of protein was loaded into each well. Following electrophoresis, gels were fixed, stained with CBB R-250, dried, and exposed to an imaging plate (BAS-MS2040; Fuji Film) for 12−24 h. The radiolabeled ND1 subunit was visualized with a Bio-Imaging Analyzer FLA-2000 (Fuji Film). For analysis of the labeled protein band, the gels were cut into 2 mm slices, and radioactivity was quantified using the γ-counting system (Packard, MINAXI γ-5550).

RESULTS

Structure−Activity Relationship for the Left-Hand Portion of the Inhibitors. Natural polyene amides have long conjugated double bonds in the left-hand portion. To elucidate the role of this portion in the inhibitory action, we first synthesized a series of derivatives having four, three, or two conjugated double bonds with a total of 16 carbon atoms (compounds **1**−**5**). The right-hand portion was set to be identical to that of natural polyene amides, i.e., (1′*S*)-2′-hydroxy-1′-methylethyl amide. The inhibitory activity of all test compounds in terms of the IC_{50}, which is a molar concentration needed to halve the control enzyme activity, was evaluated with NADH oxidase activity in SMP. As

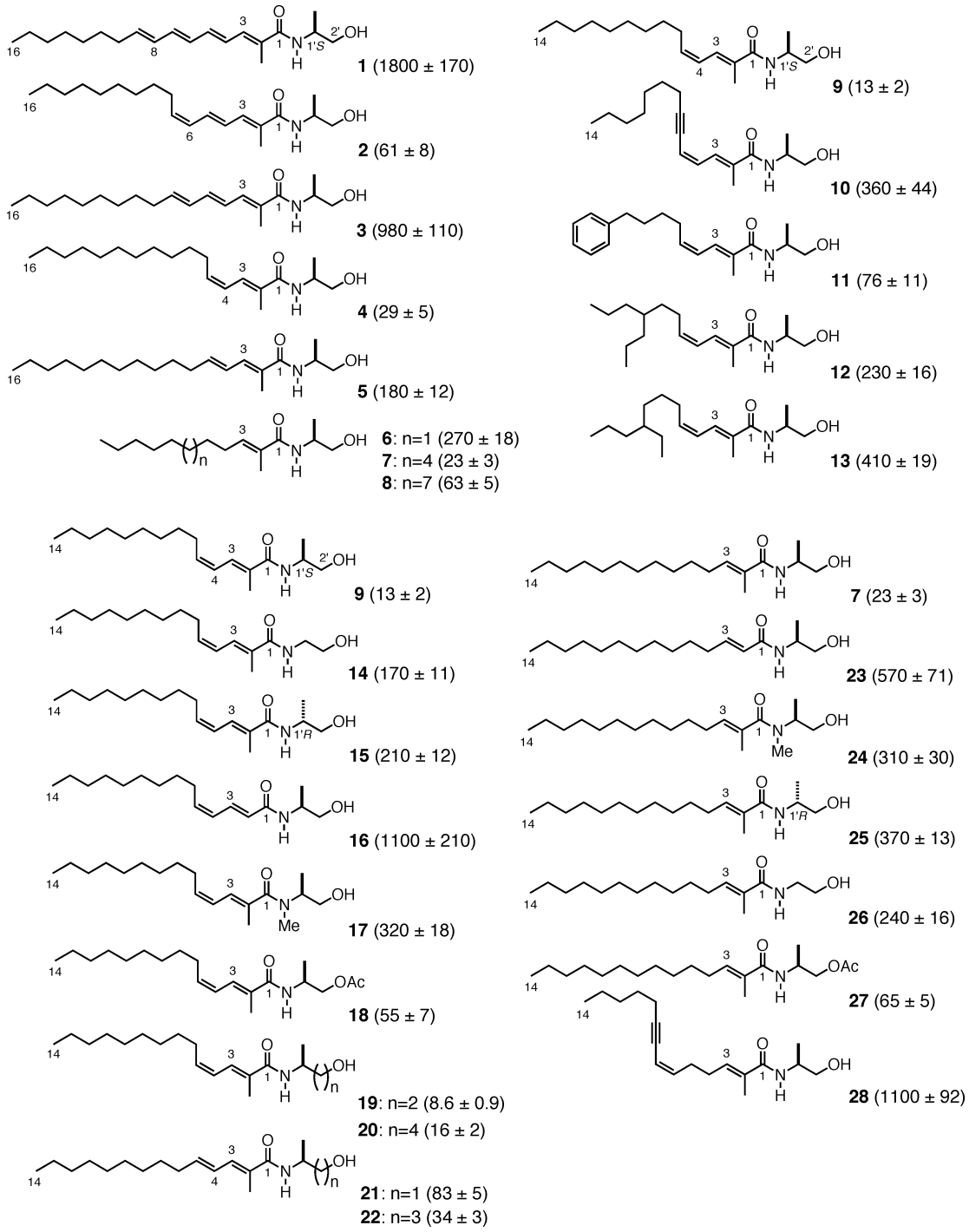

FIGURE 2: Structures of polyene amide derivatives synthesized in this study. The figures in parentheses are IC_{50} values, which are the molar concentrations needed to reduce the control NADH oxidase activity [0.61−0.70 μmol of NADH min^{-1} (mg of protein)$^{-1}$] in SMP by half. Values are means ± SD of three independent experiments. Parent compounds **7** and **9** are listed twice in this figure for the sake of comparison.

shown in Figure 2, the longer the length of the conjugated system, the weaker the potency became. *Z* geometry at the terminal of conjugated double bonds was significantly favorable for the activity compared to *E* geometry (**2** vs **3** and **4** vs **5**). The diene derivative with 2-*E*, 4-*Z* geometry (**9**) was considerably stronger than the monoene derivative (**7**), as discussed later. We were unable to evaluate the activity of natural polyene amides since these are not commercially available. However, Friedrich et al. (*9*) reported that myxalamide PI and phenalamide A_2 are about 50-fold less active than rotenone with complex I in bovine heart SMP. The IC_{50} of rotenone under our experimental conditions was 5.3 (±0.4) nM. Taking the results reported by Friedrich et al. as a reference,[2] the inhibitory effect of diene derivative **4** can be considered to be significantly stronger than that of natural polyene amides.

[2] In the introductory section, we stated that "the question of whether past studies (*1*, *9*) on the inhibition of complex I using natural polyene amides really evaluated the activity of pure individual samples would be posed". However, so long as we cannot use natural products, we have to cite the published data for reference.

Next we examined the effect of the total number of carbon atoms of the left-hand portion on the inhibitory potency using compounds **6** (C_{11}), **7** (C_{14}), and **8** (C_{17}). Both elongation and shortening of the chain from 14 carbons (**7**) resulted in a decrease in the activity, indicating that there is an optimum length (hydrophobicity) of the carbon chain for the activity. A similar tendency is generally observed for other hydrophobic inhibitors such as acetogenins (*19*, *29*). An excessive increase in the hydrophobicity of the chain may actually be adverse to the activity due to some sort of trapping in the hydrophobic lipid bilayer of the membrane.

On the basis of the above results, we fixed the total number of carbon atoms in the left-hand portion at 14 with 2-*E*, 4-*Z* geometry, as in **9**, and examined the effect of the bulkiness of this portion on the activity. The rigid (**10** and **11**) and branched (**12** and **13**) side chains were shown to be significantly unfavorable for the inhibitory action compared to the *n*-alkyl derivative (**9**) probably due to steric congestion arising from this portion. It should be mentioned that when the total number of carbon atoms in the left-hand portion was fixed at 14, *Z* geometry at the terminal of the conjugated diene was also favorable for the activity compared to *E* geometry (**9** vs **21**), as observed for **4** vs **5**.

Structure−Activity Relationship for the Right-Hand Portion of the Inhibitors. We next examined the role of the right-hand portion of the inhibitor, fixing the left-hand portion as identical to that of the most potent derivative **9**. Comparison of (*S*)-1′-methyl (**9**), 1′-H (**14**), and (*R*)-1′-methyl (**15**) derivatives showed that the presence of an (*S*)-methyl group in the 1′-position is crucial for the activity. Deletion of the 2-methyl group resulted in a drastic decrease in the activity (**9** vs **16**). Moreover, N-methylation of amide nitrogen also resulted in a remarkable decrease in the activity (**9** vs **17**), suggesting that the NH may serve as a hydrogen bond donor.

Unexpectedly, the extent of the decrease in activity caused by acetylation of the 2′-OH group (**18**) was moderate compared to that induced by the structural modifications described above, suggesting that the hydrogen bond donating ability of the 2′-OH group is not crucial for the activity. To verify this, we prepared two derivatives (**19** and **20**) in which the distance between the OH and the amide groups is elongated by one and three carbon atoms, respectively. The former (**19**) exhibited slightly stronger activity than the mother compound **9**, and the latter (**20**) still retained potent activity. A similar phenomenon was observed for the derivatives of 2-*E*, 4-*E* geometry (**21** vs **22**). These findings mean that the 2′-OH group is not involved in strict interaction with the enzyme.

One cannot exclude the possibility that the roles of the functional groups of the right-hand portion vary depending upon the structure of the left-hand portion. Therefore, we also synthesized a series of derivatives (compounds **7**, **23**−**27**) in which the left-hand portion was fixed as a monoene structure and the same structural modifications as described above were performed on the right-hand portion. Again, the crucial roles of the 2-methyl (**23**), amide NH (**24**), and 1′-(*S*)-methyl (**25** and **26**) groups were confirmed. The extent of the decrease in activity caused by acetylation of the 2′-OH group (**7** vs **27**) was moderate, as observed for **18**. Introduction of a rigid enyne unit (−C═C−C≡C−) into the left-hand portion (**28**) resulted in a great loss of activity.

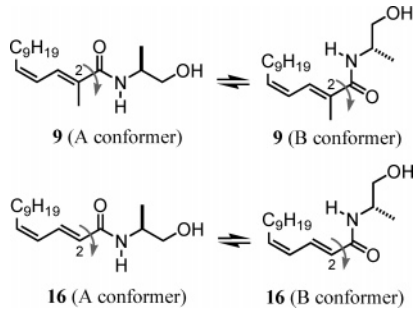

FIGURE 3: Two possible extreme conformers (A and B) of compounds **9** and **16**. The two conformers are interconverted by rotation through 180° around the bond indicated by the gray arrows.

Effect of N-Methyl and 2-Methyl Groups on Inhibitor Conformation. Both N-methylation (**17** and **24**) and deletion of the 2-methyl group (**16** and **23**) drastically reduced the inhibitory activity. Since the marked decrease in activity would be associated with significant conformational changes of the compounds, we analyzed the effects of structural modifications on the inhibitor conformation in this section.

When the ^{1}H NMR spectrum of **17** was measured in chloroform-d_1 at 25 °C for identification of the compound's structure, broad signals at 4.52 and 3.62 ppm assigned to the 1′-methyne and 2′-methylene protons, respectively, were recorded. In contrast, ^{1}H NMR spectra of other related derivatives showed a sharp multiplet signal for the 1′-methyne proton and two double-doublet signals for the 2′-methylene protons. These observations suggest that rotational motion around the CO−NH bond of **17** is somewhat restricted. To better elucidate the effect of N-methylation on the conformation of **17**, we examined the effect of temperature on the ^{1}H NMR spectrum using methanol-d_4 in place of chloroform-d_1. At 25 °C, split broad signals assigned to the 1′-metyne proton were observed at 4.59 and 4.11 ppm in a ratio of 0.3:0.7, and two broad signals assigned to the 2′-methylene protons were observed at 3.58 and 3.46 ppm in a ratio of 1.3:0.7. In addition, a broad signal assigned to the *N*-methyl protons appeared at 2.83 ppm. Upon increasing the temperature to 50 °C, the two signals of the 1′-metyne proton coalesced, giving a broad single resonance at 4.28 ppm, and the two broad signals for the 2′-methylene protons changed to two multiplet signals in a ratio of 1:1. The broad signal of the *N*-methyl protons significantly sharpened. These results mean that the rotational energy of the CO−NH bond increases with N-methylation of the amide nitrogen. Accordingly, although we pointed out the importance of the hydrogen bond donating ability of the NH group in the above section, we cannot completely exclude the possibility that the marked decrease in activity caused by N-methylation is due to a loss of rotational freedom of the CO−NH bond to take an active conformation.

The drastic decrease in the activities of **16** and **23** suggests that the 2-methyl group may adjust an active conformation of the α,β-unsaturated carbonyl moiety. To elucidate the role of the 2-methyl group, we considered the pair **9** and **16** below. Two extreme conformations of this moiety may be supposed, as shown in Figure 3. From ^{1}H NMR measurement of **9** in chloroform-d_1, a NOE was observed between the 2-methyl and NH protons. A similar NOE was reported for natural stipiamide in acetone-d_6 (*20*), indicating that a conformation close to conformer A is predominant in organic

Table 1: Comparison of the Inhibitory Effect on Forward and Reverse Electron Transfer Activities

	IC_{50} values (pmol of inhibitor/mg of protein)[a]	
inhibitor	forward electron transfer	reverse electron transfer
compound **9**	433 ± 66	850 ± 110
rotenone	157 ± 16	75 ± 7
bullatacin	46 ± 5[b]	28 ± 4[b]
piericidin A	81 ± 7[b]	48 ± 4[b]

[a] Values are means ± SD of three independent experiments. [b] From ref *30*.

solvent probably due to steric congestion between the 2-methyl group and the carbonyl oxygen in conformer B. Nevertheless, one cannot exclude the possibility that, concerning **16**, conformer B is more stable than conformer A because of a lack of such steric congestion. To better understand the role of the methyl group, we carried out a conformational analysis using Spartan 04 (Wavefunction, Inc.). The Monte Carlo calculation using MMFF94 showed that the most stable conformation of **9** and **16** is close to conformer B rather than conformer A (see Supporting Information). However, the calculated rotational energy barrier around the bond marked by a gray arrow in Figure 3 is low for both compounds, being 2−3 kcal/mol. This result means that interconversion of conformers A ⇔ B takes place readily at the assay temperature irrespective of the presence of the 2-methyl group. Taking into consideration the results of the theoretical calculation, a difference in the conformational property of this portion may not be the cause, at least not the main cause, of the weak activity of **16** and **23**. Although we cannot presume which conformer is close to an active conformation in the enzyme-bound state, the presence of a methyl group at the 2-positoin is crucial for the activity probably to support tight hydrogen bonding of the amide group to the enzyme.

Action Mechanism. In view of the unique chemical nature of the polyene amides, it was of interest to determine whether their inhibition manner differs from that of other traditional complex I inhibitors such as rotenone and piericidin A. Therefore, using compound **9** as representative of the polyene amides, we characterized in detail the mode of inhibition by focusing on the following three points: (i) effects on the reverse electron transfer (i.e., ubiquinol−NAD^+ oxidoreductase activity in the presence of protonmotive force), (ii) induction of superoxide production, and (iii) suppression of the specific photoaffinity labeling of the ND1 subunit by a photoreactive acetogenin derivative, [^{125}I]TDA (*24*).

First, we measured the inhibition of the reverse electron transfer in complex I by **9**. The IC_{50} values (picomoles of inhibitor per milligram of protein) for the forward and reverse electron transfer are listed in Table 1, including rotenone, piericidin A, and bullatacin as a reference. A direct comparison of the IC_{50} values between the two assays is complicated since a higher concentration of SMP was used in the reverse electron transfer assay (0.1 vs 0.03 mg of protein/mL), resulting in an increase in volume of the membrane lipid phase as well as the concentration of complex I (*30*). Nevertheless, when the activities of various inhibitors in terms of the IC_{50} values were compared for convenience (Table 1), it was found that rotenone, piericidin A, and bullatacin block the reverse electron transfer more efficiently than the forward electron transfer, whereas an opposite phenomenon was observed for **9**, indicating a direction-specific effect. A similar phenomenon was reported for Δlac-acetogenins, a new type of complex I inhibitor (*24*, *30*).

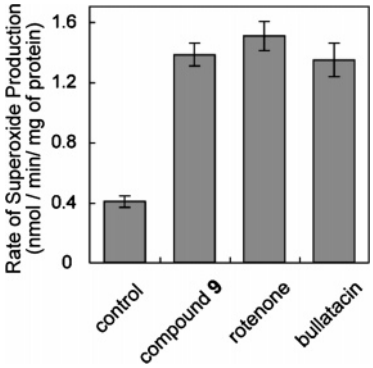

FIGURE 4: Superoxide production from complex I in the presence of inhibitor. Rates of superoxide production in the NADH oxidase assay were determined with SMP. Where indicated, 13 μM compound **9**, 1.2 μM rotenone, or 1.2 μM bullatacin was added. The concentrations of all inhibitors were set high enough to achieve complete inhibition of NADH oxidase activity. The final mitochondrial protein concentration is 0.25 mg of protein/mL. Bars show means ± SD of three independent measurements.

We next determined superoxide production from complex I induced by **9**. The main reductant of oxygen producing superoxide in complex I has not been identified, and published results are highly conflicting (i.e., FMN, iron−sulfur centers, or ubisemiquinone). One possible cause of this is that the superoxide generation from the enzyme varies greatly depending on the tissue, species, and experimental conditions (*31*−*33*). However, a comparison of the superoxide production induced by different inhibitors is helpful to know whether the effect of the inhibitors on the reductant (i.e., the free radical intermediate) or its environment is similar (*34*). We compared the rate of superoxide production induced by **9**, rotenone, or bullatacin at a concentration range high enough to achieve maximum inhibition of NADH oxidase activity. The rate of superoxide production induced by **9** was comparable to that induced by rotenone and bullatacin (Figure 4), indicating that the effects of the inhibitors on the free radical intermediate are not largely different.

Finally, we examined the suppressive effect of **9** on the specific photoaffinity labeling of the ND1 subunit by an acetogenin derivative, [^{125}I]TDA. We recently showed that [^{125}I]TDA specifically labels the ND1 subunit upon UV irradiation and this labeling is completely suppressed by numerous other complex I inhibitors (*24*). As shown in Figure 5, compound **9** also blocked the labeling of ND1 in a concentration-dependent manner. The complete suppression by **9** could not be determined because of the solubility limit above ∼10^4 nM. Much higher concentrations of **9** than piericidin A were needed to suppress the labeling. This is due to a lower affinity of **9** for complex I, as expected from the IC_{50} values: 1.2 (±0.09) and 13 (±2.0) nM for piericidin A and **9**, respectively.[3] It is concluded that the binding site of **9** is identical or at least near to that of other complex I inhibitors, which are believed to share a common large binding domain with partially overlapping sites (*9*, *24*, *35*).

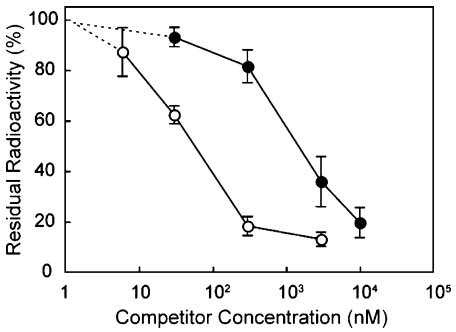

FIGURE 5: Effects of compound **9** and piericidin A on the specific photoaffinity labeling of the ND1 subunit by [^{125}I]TDA. A competitor was added to SMP (0.3 mg of protein/mL) at given concentrations and incubated for 10 min prior to treatment with [^{125}I]TDA (3 nM). Key: compound **9** (closed circles) and piericidin A (open circles). Data are the mean of three independent measurements ± SD.

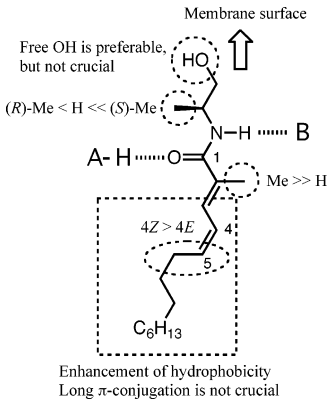

FIGURE 6: A summary of SAR study of synthetic polyene amides is illustrated, taking compound **9** as an example. The hydrogen-bonding ability of the amide group is the only crucial factor deciding tight binding to the enzyme (AH, hydrogen-bonding donor; B, hydrogen-bonding acceptor), and other functional groups including the hydrophobic left-hand portion serve to effect the hydrogen-bonding ability.

DISCUSSION

The results of the SAR study of the polyene amides are summarized in Figure 6, taking compound **9** as an example. With respect to the left-hand portion of the inhibitor, the extended π-conjugation system is not required for the inhibition. The conjugated diene (−C═C−C═C−CO−) was shown to substitute for the natural polyene skeleton to retain the function. The primary role of this portion must be an enhancement of the hydrophobicity of the molecule to make the partitioning into the hydrophobic environment of the enzyme favorable energetically. This notion is consistent with the fact that the presence of a hydroxy group at the C13-position is common to many natural polyene amides (see Figure 1), whereas this group is not essential for antifungal activity against *Phytophthora capsici* (*3*). It is clear, however, that the geometry of the C4/C5 double bond and the width of this portion were strictly recognized by the enzyme. It is therefore likely that the left-hand portion binds to a narrow hydrophobic pocket in the enzyme rather than merely partitioning into the lipid membrane phase. In this connection, it should be noted that the truncated 6,7-dehydrostipiamide, which has a rigid enyne structure, resembling **28**, in the left-hand portion of natural stipiamide, is far less toxic to breast cancer cells than is natural stipiamide (*6*).

The right-hand portion of the molecule is a toxophore of this series of inhibitors. The presence of the 2-methyl, amide NH, and (*S*)-1′-methyl groups was revealed to be crucial for potent activity. Both methyl groups neighboring the amide group may finely adjust the hydrogen-bonding ability of the amide group. Unexpectedly, the extent of the decrease in activity caused by acetylation of the 2′-OH group (**18** and **27**) was moderate, suggesting that the free 2′-OH group is favorable, but not crucial, for potent inhibition. This idea is supported by the fact that elongation of the distance between the OH group and the amide bond did not significantly affect the activity (**9** vs **19** and **20**, and **21** vs **22**). On the basis of these findings, we propose that the role of this functional group is not to serve as a hydrogen bond donor to the enzyme but to act as a hydrophilic anchor directing the right-hand portion at or near the membrane surface. It should be noted that the free 2′-OH group is not important for antifungal activity (*3*). Taken together, it is concluded that the hydrogen-bonding ability of the amide group is the only crucial factor deciding tight binding to the enzyme, and other functional groups including the hydrophobic left-hand portion serve to effect the hydrogen-bonding ability.

Recently, the crystal structure of the hydrophilic domain (peripheral arm) of *Thermus thermophilus* complex I, where all the known cofactors of the enzyme reside, was solved at 3.3 Å resolution (*36*). However, our knowledge of the functional and structural features of the membrane arm is still highly limited (*10*−*12*). Taking into consideration the proposed dynamic function of the membrane segment of complex I in proton pumping as well as the concept of a common large inhibitor-binding domain supposed to be constructed by multisubunits (*10*−*12*), it may not be strange that there are diverse chemicals that disturb the function of the membrane domain differently depending on their structural specificity. In fact, we recently showed that Δlac-acetogenins, which were synthesized originally in our laboratory (*37*), inhibit complex I activity in a different manner from that of traditional inhibitors, though the inhibition site of Δlac-acetogenins is downstream of the iron−sulfur cluster N2, as is the case of traditional inhibitors (*24*, *38*). Therefore, the study on the action mechanism of chemically unique polyene amides was important not to overlook a possible new mechanism of inhibition. On the basis of an electron paramagnetic resonance (EPR) spectroscopic study, Friedrich et al. (*9*) demonstrated that the inhibition site of the polyene amides is downstream of the iron−sulfur cluster N2. The present study indicates that, despite their unique chemical nature, polyene amides can be considered ordinary complex I inhibitors. However, in view of the direction-specific effect of the polyene amides (Table 1), their binding position within the large inhibitor-binding domain may differ considerably from that of other complex I inhibitors.

The concept of a large inhibitor-binding domain in bovine complex I may be interpreted in analogy with the ubiquinol oxidation site (Q_o site) in the cytochrome bc_1 complex (complex III). Before crystallographic information became

[3] According to a simple bimolecular association model, a difference in the IC_{50} values suggests that the binding affinities of the two inhibitors in terms of a dissociation constant (K_d) differ by at least 10-fold (see our previous theoretical analysis published in ref *30*).

available, Q_o site inhibitors had been divided into subgroups based on biophysical and spectroscopic studies of a heme b_L and iron−sulfur cluster upon the binding of inhibitors (*41*). On the basis of the crystal structure of bovine complex III with bound inhibitors, the inhibitors of a Q_o site are divided into two subgroups, i.e., Pm and Pf inhibitors (*42*). The Pm inhibitors cause iron−sulfur protein (ISP) into a mobile conformation, whereas the Pf inhibitors force ISP into a fixed conformation. The cd1 helix of cytochrome *b* plays an important role in responding discriminately to the two types of Q_o site inhibitors. It is notable that, taking strobilurin (Pm inhibitor) and stigmatellin (Pf inhibitor) as examples of the most distant inhibitors, there is no overlap between the two toxophore groups (*42*). Turning to complex I inhibitors, several studies along with the present work suggested that the inhibition mechanisms of chemically diverse complex I inhibitors are somewhat different (*35*, *43*−*45*). It should be realized that the concept of a common large binding domain was proposed on the basis of the apparent competitive behavior among the inhibitors; namely, the binding of a marker inhibitor to complex I is suppressed by an excess amount of other complex I inhibitors (*35*, *39*, *40*). Under the experimental conditions, one cannot rule out the possibility that the competitor prevents binding of a marker ligand by inducing structural change in the enzyme, rather than by occupying the same site, as mentioned in the introductory section. Taken together, we cannot exclude the possibility that there is no overlap between some pairs of chemically diverse complex I inhibitors, as observed for the Q_o site inhibitors. The complete crystal structure of complex I is needed to understand the functions of the membrane segment of the enzyme as well as the inhibitor-binding site.

ACKNOWLEDGMENT

We thank Dr. Kazuhiro Irie, Kyoto University, for technical assistance with the NMR measurements.

SUPPORTING INFORMATION AVAILABLE

Synthetic procedures of compounds **1**−**28** and the 3D structure of the most stable conformation of compounds **9** and **16**. This material is available free of charge via the Internet at http://pubs.acs.org.

REFERENCES

1. Jansen, K. G. R., Reifenstahl, G., Höfle, G., irshik, H., Kunze, B., Reichenbach, H., and Thierbach, G. (1983) The myxalamides, new antibiotics from *Myxococcus xanthus* (myxobacterales), *J. Antibiot. 36*, 1150−1157.
2. Andrus, M. B., and Lepore, S. D. (1997) Synthesis of stipiamide and a new multidrug resistance reversal agent, 6,7-dehydrostipiamide, *J. Am. Chem. Soc*. *119*, 2327−2328.
3. Kundim, B. A., Utou, Y., Sakagami, Y., Fudou, R., Yamanaka, S., and Ojika, M. (2004) Novel antifungal polyene amides from the myxobacterium *Cystobacter fuscus*: isolation, antifungal activity and absolute structure determination, *Tetrahedron 60*, 10217−10221.
4. Walker, J. E. (1992) The NADH-ubiquinone oxidoreductase (complex I) of respiratory chains, *Q. Rev. Biophys. 25*, 253−324.
5. Andrus, M. B., Lepore, S. D., and Turner, T. M. (1997) Total synthesis of stipiamide and designed polyenes as new agents for the reversal of multidrug resistance, *J. Am. Chem. Soc*. *119*, 12159−12169.
6. Mapp, A. K., and Heathcock, C. H. (1999) Total synthesis of myxalamide A, *J. Org. Chem*. *64*, 23−27.
7. Hoffmann, R. W., Rohde, T., Haeberlin, E., and Schäfer, F. (1999) Total synthesis of phenalamide A_2, *Org. Lett. 1*, 1713−1715.
8. Coleman, R. S., Lu, X., and Modolo, I. (2007) Total synthesis of 2′-*O*-methylmyxalamide D and (6*E*)-2′-*O*-methylmyxalamide D, *J. Am. Chem. Soc*. *129*, 3826−3827.
9. Friedrich, T., Van Heek, P., Leif, H., Ohnishi, T., Forche, E., Kunze, B., Jansen, R., Trowitzsch-Kienast, W., Höfle, G., Reichenbach, H., and Weiss, H. (1994) Two binding sites of inhibitors in NADH-ubiquinone oxidoreductase (complex I), *Eur. J. Biochem. 219*, 691−698.
10. Yagi, T., and Matsuno-Yagi, A. (2003) The proton-translocating NADH-quinone oxidoreductase in the respiratory chain: the secret unlocked, *Biochemistry 42*, 2266−2274.
11. Hirst, J. (2005) Energy transduction by respiratory complex I; an evaluation of current knowledge, *Biochem. Soc. Trans*., 525−529.
12. Brandt, U. (2006) Energy converting NADH-quinone oxidoreductase (complex I), *Annu. Rev. Biochem. 75*, 69−92.
13. Satoh, T., Miyoshi, H., Sakamoto, K., and Iwamura, H. (1996) Comparison of the inhibitory action of synthetic capsaicin analogues with various NADH-ubiquinone oxidoreductases, *Biochim. Biophys. Acta 1273*, 21−30.
14. Yabunaka, H., Kenmochi, A., Nakatogawa, A., Sakamoto, K., and Miyoshi, H. (2002) Hybrid ubiquinone; novel inhibitor of mitochondrial complex I, *Biochim. Biophys. Acta 1556*, 106−112.
15. Ueno, H., Miyoshi, H., Ebisui, K., and Iwamura, H. (1994) Comparison of the inhibitory action of natural rotenone and its stereoisomers with various NADH-ubiquinone reductases, *Eur. J. Biochem. 225*, 411−417.
16. Ueno, H., Miyoshi, H., Inoue, M., Niidome, Y., and Iwamura, H. (1996) Structural factors of rotenone required for inhibition of various NADH-ubiquinone oxidoreductases, *Biochim. Biophys. Acta 1276*, 195−202.
17. Kuwabara, K., Takada, M., Iwata, J., Tatsumoto, K., Sakamoto, K., Iwamura, H., and Miyoshi, H. (2000) Design syntheses and mitochondrial complex I inhibitory activity of novel acetogenin mimics, *Eur. J. Biochem. 267*, 2538−2546.
18. Takada, M., Kuwabara, K., Nakato, H., Tanaka, A., Iwamura, H., and Miyoshi, H. (2000) Definition of crucial structural factors of acetogenins, potent inhibitors of mitochondrial complex I, *Biochim. Biophys. Acta 1460*, 302−310.
19. Abe, M., Murai, M., Ichimaru, N., Kenmochi, A., Yoshida, T., Kubo, A., Kimura, Y., Moroda, A., Makabe, H., Nishioka, T., and Miyoshi, H. (2005) Dynamic function of the alkyl spacer of acetogenins in their inhibitory action with mitochondrial complex I (NADH-Ubiquinone Oxidoreductase), *Biochemistry 44*, 14898−14906.
20. Kim, Y. J., Furuhata, K., Yamanaka, S., Fudo, R., and Seto, H. (1991) Isolation and structural elucidation of stipiamide, a new antibiotic effective to multidrug-resistant cancer cells, *J. Antibiot. 44*, 553−556.
21. Andrus, M. B., Turner, T. M., Asgari, D., and Li, W. (1999) The synthesis and evaluation of a solution-phase indexed combinatorial library of non-natural polyenes for multidrug resistance reversal, *J. Org. Chem. 64*, 2978−2979.
22. Andrus, M. B., Turner, T. M., Sauna, Z. E., and Ambudkar, S. V. (2000) The synthesis and evaluation of a solution phase indexed combinatorial library of non-natural polyenes for reversal of P-glycoprotein mediated multidrug resistance, *J. Org. Chem. 65*, 4973−4983.
23. Sauna, Z. E., Andrus, M. B., Turner, T. M., and Ambudkar, S. V. (2004) Biochemical basis of polyvalency as a strategy for enhancing the efficacy of P-glycoprotein (ABCB1) modulators: stipiamide homodimers separated with defined-length spacer reverse drug efflux with greater efficacy, *Biochemistry 43*, 2262−2271.
24. Murai, M., Ishihara, A., Nishioka, T., Yagi, T., and Miyoshi, H. (2007) The ND1 subunit constructs inhibitor binding domain in bovine heart mitochondrial complex I, *Biochemistry 46*, 6409−6416.
25. Matsuno-Yagi, A., and Hatefi, Y. (1985) Studies on the mechanism of oxidative phosphorylation, *J. Biol. Chem. 260*, 14424−14427.
26. Boveris, A. (1984) Determination of the production of superoxide radicals and hydrogen peroxide in mitochondria, *Methods Enzymol. 105*, 429−435.
27. Ernster, L., and Lee, C.-P. (1967) Energy-linked reduction of NAD^+ by succinate, *Methods Enzymol. 10*, 729−738.
28. Laemmli, U. K. (1970) Cleavage of structural proteins during the assembly of the head of bacteriophage T4, *Nature 227*, 680−685.

29. Miyoshi, H., Ohshima, M., Shimada, H., Akagi, T., Iwamura, H., and McLaughlin, J. L. (1998) Essential structural factors of annonaceous acetogenins as potent inhibitors of mitochondrial complex I, *Biochim. Biophys. Acta 1365*, 443−452.
30. Murai, M., Ichimaru, N., Abe, M., Nishioka, T., and Miyoshi, H. (2006) Mode of inhibitory action of Δlac-acetogenins, a new class of inhibitors of bovine heart mitochondrial complex I, *Biochemistry 45*, 9778−9787.
31. Herrero, A., and Barja, G. (2000) Localization of the site of oxygen radical generation inside the complex I of heart and nonsynaptic brain mammalian mitochondria, *J. Bioenerg. Biomembr. 32*, 609−615.
32. Liu, Y., Fiskum, G., and Schubert, D. (2002) Generation of reactive oxygen species by the mitochondrial electron transport chain, *J. Neurochem. 80*, 780−787.
33. Lambert, A. J., and Brand, M. D. (2004) Superoxide production by NADH:ubiquinone oxidoreductase (complex I) depends on the pH gradient across the mitochondrial inner membrane, *Biochem. J. 382*, 511−517.
34. Lambert, A. J., and Brand, M. D. (2004) Inhibitors of the quinone-binding site allow rapid superoxide production from mitochondrial NADH-ubiquinone oxidoreductase (complex I), *J. Biol. Chem. 279*, 39414−39420.
35. Okun, J. G., Lümmen, P., and Brandt, U. (1999) Three classes of inhibitor share a common binding domain in mitochondrial complex I (NADH-ubiquinone oxidoreductase), *J. Biol. Chem. 274*, 2625−2630.
36. Sazanov, L. A., and Hinchliffe, P. (2006) Structure of the hydrophilic domain of respiratory complex I from *Thermus thermophilus*, *Science 311*, 1430−1436.
37. Hamada, T., Ichimaru, N., Abe, M., Fujita, D., Kenmochi, A., Nishioka, T., Zwicker, K., Brandt, U., and Miyoshi, H. (2004) Synthesis and inhibitory action of novel acetogenin mimics with bovine heart mitochondrial complex I, *Biochemistry 43*, 3651−3658.
38. Ichimaru, N., Murai, M., Abe, M., Hamada, T., Yamada, Y., Makino, S., Nishioka, T., Makabe, H., Makino, A., Kobayashi, T., and Miyoshi, H. (2005) Synthesis and inhibition mechanism of Δlac-acetogenins: a novel type of inhibitor of bovine heart mitochondrial complex I, *Biochemistry 44*, 816−825.
39. Schuler, F., Yano, T., Bernardo, S. D., Yagi, T., Yankovskaya, V., Singer, T. P., and Casida, J. E. (1999) NADH-quinone oxidoreductase: PSST subunit couples electron transfer from iron-sulfur cluster N2 to quinone, *Proc. Natl. Acad. Sci. U.S.A. 96*, 4149−4153.
40. Nakamaru-Ogiso, E., Sakamoto, K., Matsuno-Yagi, A., Miyoshi, H., and Yagi, T. (2003) The ND5 subunit was labeled by a photoaffinity analogue of fenpyroximate in bovine mitochondrial complex I, *Biochemistry 42*, 746−754.
41. Von, Jagow, G., and Link, T. A. (1986) Use of specific inhibitors on the mitochondrial bc_1 complex, *Methods Enzymol. 126*, 253−271.
42. Esser, L., Quinn, B., Li, Y.-F., Zhang, M., Elberry, M., Yu, L., Yu, C.-A., and Xia, D. (2004) Crystallographic studies of quinol oxidation site inhibitors: a modified classification of inhibitors for the cytochrome bc_1 complex, *J. Mol. Biol. 341*, 281−302.
43. Kotlyar, A. B., and Gutman, M. (1992) The effect of $\Delta\mu_{H^+}$ on the interaction of rotenone with complex I of submitochondrial particles, *Biochim. Biophys. Acta 1140*, 169−174.
44. Schuler, F., and Casida, J. E. (2001) Functional coupling of PSST and ND1 sununits in NADH-ubiquinone oxidoreductase established by photoaffinity labeling, *Biochim. Biophys. Acta 1506*, 79−87.
45. Ohnishi, S. T., Ohnishi, T., Muranaka, S., Fujita, H., Kimura, H., Uemura, K., Yoshida, K., and Utsumi, K. (2005) A possible site of superoxide generation in the complex I segment of rat heart mitochondria, *J. Bioenerg. Biomembr. 37*, 1−15.

BI7010306